# Methyl CpG–binding proteins induce large-scale chromatin reorganization during terminal differentiation

Alessandro Brero,[1,2] Hariharan P. Easwaran,[2] Danny Nowak,[2] Ingrid Grunewald,[2] Thomas Cremer,[1] Heinrich Leonhardt,[1,2] and M. Cristina Cardoso[2]

[1]Department of Biology II, Ludwig Maximilians University Munich, 82152 Planegg-Martinsried, Germany
[2]Max Delbrück Center for Molecular Medicine, 13125 Berlin, Germany

Pericentric heterochromatin plays an important role in epigenetic gene regulation. We show that pericentric heterochromatin aggregates during myogenic differentiation. This clustering leads to the formation of large chromocenters and correlates with increased levels of the methyl CpG–binding protein MeCP2 and pericentric DNA methylation. Ectopic expression of fluorescently tagged MeCP2 mimicked this effect, causing a dose-dependent clustering of chromocenters in the absence of differentiation. MeCP2-induced rearrangement of heterochromatin occurred throughout interphase, did not depend on the H3K9 histone methylation pathway, and required the methyl CpG–binding domain (MBD) only. Similar to MeCP2, another methyl CpG–binding protein, MBD2, also increased during myogenic differentiation and could induce clustering of pericentric regions, arguing for functional redundancy. This MeCP2- and MBD2-mediated chromatin reorganization may thus represent a molecular link between nuclear genome topology and the epigenetic maintenance of cellular differentiation.

## Introduction

Most studies trying to understand how, during development, a multitude of different cell types with specific phenotypes and functions can arise from a pluripotent state have focused on transcriptional activation. The latter would, in a sequential manner, commit the cell to a specific lineage. Another view considers cellular differentiation as a progression of silencing events leading to an increasing inactivation of the genome. There is augmenting evidence in favor of gene silencing as cell fate determinant (for review see Fisher and Merkenschlager, 2002). Studies in yeast (Maillet et al., 1996), *Drosophila* (Dernburg et al., 1996), and in mammals (Brown et al., 1997) have provided strong evidence for a role of nuclear topology, in particular heterochromatin proximity (in cis or in trans), in transcriptional silencing (for review see Kosak and Groudine, 2004).

In mammals, heterochromatin is characterized by high levels of specifically methylated forms of histone H3, deacetylated histone H4, and DNA methylation. Both methylation of histone H3 (at lysine 9) and methylation of cytosines (at CpG dinucleotides) are binding sites for chromatin modifiers such as the HP1 proteins and the methyl CpG–binding domain (MBD) proteins, respectively. The latter "translate" the DNA methylation signal into transcriptional repression at least partially by recruiting silencing complexes and histone deacetylases, thereby stabilizing and consolidating the heterochromatic state (for review see Bird and Wolffe, 1999; Leonhardt and Cardoso, 2000). Both HP1 (Furuta et al., 1997) and MeCP2 (Lewis et al., 1992) (the founding member of the MBD family) have been shown to be highly concentrated at pericentric heterochromatin. Binding of MeCP2 to pericentric heterochromatin is dependent on DNA methylation and requires the MBD (Nan et al., 1996). Mutations in the MeCP2 gene were linked to Rett syndrome, a common neurodevelopmental disorder in humans (Amir et al., 1999). The MeCP2 protein level has been shown to increase during neuronal differentiation (Jung et al., 2003) and was suggested to be critical for synaptogenesis (Mullaney et al., 2004), maturation, and maintenance of neurons (Kishi and Macklis, 2004).

Studies on mouse neurons (Manuelidis, 1985; Martou and De Boni, 2000; Solovei et al., 2004) indicated a specific rearrangement of centromeric domains in terminally differentiated cells. We have set out to test whether large-scale reorganization of heterochromatin within the nucleus is a feature of terminal differentiation and whether histone H3K9 or DNA methylation and its translation by MBD proteins play an important role in this process.

Correspondence to M. Cristina Cardoso: cardoso@mdc-berlin.de

Abbreviations used in this paper: coRID, corepressor interacting domain; MBD, methyl CpG–binding domain; TRD, transcriptional repressor domain.

The online version of this article includes supplemental material.


The Journal of Cell Biology, Vol. 169, No. 5, June 6, 2005 733–743
http://www.jcb.org/cgi/doi/10.1083/jcb.200502062

Supplemental Material can be found at:
http://www.jcb.org/cgi/content/full/jcb.200502062/DC1

## Results

### MeCP2 expression and pericentric DNA methylation increase during myogenesis

To elucidate epigenetic changes taking place during cellular differentiation, we tested whether DNA methylation and expression of its binding factor MeCP2 correlated with differentiation. For that purpose, we made use of a well-established in vitro culture system for muscle differentiation. Pmi28 primary myoblasts (Kaufmann et al., 1999) or the C2C12 myoblast cell line (Yaffe and Saxel, 1977) were induced to undergo myogenic differentiation by incubating the cultures with horse serum containing medium. After 3–4 d, the cells formed polynucleated syncitial myotubes with a few still-mononucleated cells (myocytes) that expressed muscle-specific markers (unpublished data). Recent studies have shown that MeCP2 expression increases during neuronal differentiation in humans (LaSalle et al., 2001), rats (Jung et al., 2003), and mice (Cohen et al., 2003). To test whether MeCP2 levels would also increase during myogenesis, we compared endogenous MeCP2 levels in myoblasts versus myotubes by immunofluorescence and Western blotting. In myoblast cultures only 11% of the cells analyzed exhibited the typical MeCP2 pattern at pericentric heterochromatin (Fig. 1 B), whereas in myotubes almost all nuclei (99%) showed MeCP2 staining (Fig. 1, A and C). In myocytes, 75% showed detectable MeCP2 at pericentric sites, suggesting that the increase of MeCP2 protein is gradual during differentiation and precedes myotube formation. The dramatic increase in MeCP2 expression demonstrated in situ by immunofluorescence could be corroborated by Western blot analysis. Equivalent amounts of total nuclear protein from cultures of undifferentiated myoblasts and terminally differentiated myotubes was compared and, as shown in Fig. 1 D, the MeCP2 level was undetectable in proliferating myoblasts but highly enriched in myotubes.

We then investigated the level and localization of methylated CpGs (5mC) to which MeCP2 selectively binds in myoblasts versus myotubes using specific antibodies, as well as by Southern blot analysis using methylation sensitive restriction enzyme digestion of genomic DNA. Intensive antibody staining of pericentric heterochromatin was observed in an increasing percentage of nuclei from myoblasts (23%) over myocytes (54%) to myotubes (70%), thus paralleling the MeCP2 results (Fig. 1 C). The lack of detectable antibody staining in a substantial part of cells in all three populations is most likely due to lower DNA methylation levels that are below the detection threshold of the in situ immunological procedure. In fact, digestion of genomic DNA with the methylation-sensitive restriction enzyme HpyCH4 IV and subsequent Southern blot analysis showed general methylation of the major satellite regions in myoblasts, albeit to a reproducible lesser extent than in myotubes (Fig. 1 E) corroborating these in situ results.

### Clustering of pericentric heterochromatin during terminal differentiation

Because MeCP2 and DNA methylation have been implicated in heterochromatin formation and maintenance, we tested whether pericentric heterochromatin, which is highly enriched in both, undergoes structural changes during differentiation. To visualize the nuclear organization of pericentric heterochromatin during terminal differentiation, we used 3D-FISH (Solovei et al., 2001) with a major satellite-specific probe. Mouse pericentric heterochromatin consists of large arrays of tandem major satellite repeats. It accounts for ~10% of the genome (Mitchell, 1996) and shows a tendency to form clusters, so-called chromocenters (Hsu et al., 1971). The mean number of chromocenters in terminally differentiated cells (11.1) versus undifferentiated precursors (20.4) was markedly reduced (Fig. 2), whereas the size of the clusters increased concomitantly. The decrease in numbers was statistically highly significant ($P < 0.001$). Moreover, the variability in chromocenter number within myotube nuclei diminished, as the SD dropped from 6.1 to 2.9 (Fig. S1, available



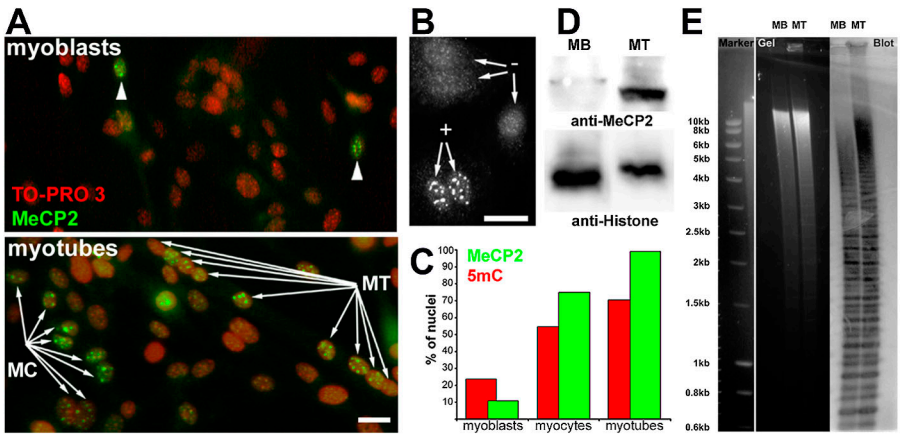


Figure 1. **MeCP2 level increases during myogenesis and is paralleled by an increased methylation of pericentric DNA.** (A) Undifferentiated and differentiated Pmi28 cultures were immunolabeled for MeCP2 (green) and counterstained with TO-PRO3 (red). Panels in A show two equally sized areas of an undifferentiated myoblast culture (top) and of a culture 3 d after induction of differentiation (bottom). Although in the myoblast culture only two cells show MeCP2 staining (arrowheads), in the differentiated culture many myocytes (MC) and almost all myotube nuclei (MT) are stained (arrows). Bar, 20 μm. 230 myoblast, 220 myocyte, and 214 myotube nuclei were scored for detectable MeCP2 signals. B exemplifies the scoring on five myocyte nuclei: three nuclei show no detectable MeCP2 signals (−), whereas two exhibit the characteristic MeCP2 pattern (+) with most of the protein being localized at pericentric heterochromatin. Bar, 20 μm. (C) The histogram summarizes the quantification of detectable MeCP2 signals and of highly methylated DNA in pericentric regions of myoblast, myocytes, and myotubes. DNA methylation was assessed using an mAb against 5-methyl-cytosine (5mC). Scoring was performed as for MeCP2. (D) A Western blot analysis comparing endogenous protein levels of MeCP2 in C2C12 myoblasts versus myotubes. Histone level was used as control for loading of nuclear proteins. (E) Southern blot analysis of genomic DNA from myoblasts (MB) versus myotubes (MT) digested with the methylation-sensitive restriction enzyme HpyCH4 IV (5′-ACGT-3′). Digested DNA was probed with a major satellite-specific probe. Note the higher concentration of undigested high molecular weight DNA in the myotube sample, indicating an increased methylation level.

at http://www.jcb.org/cgi/content/full/jcb.200502062/DC1). This substantial increase in heterochromatin clustering is probably a continuous process in myoblast-to-myotube transition, as myocytes, which represent an intermediate differentiation state, showed an intermediate number of chromocenters (average 14.5 SD = 4.4; see Fig. 5 B and Fig. S1).

We observed such an increased clustering of pericentric heterochromatin also during terminal differentiation of mouse embryonic stem cells to macrophages (unpublished data). Moreover, this phenomenon has been reported in other cell lineages and species (human neutrophils [Beil et al., 2002]; human and mouse neurons [Manuelidis, 1985; Martou and De Boni, 2000; Solovei et al., 2004]; rat myoblasts [Chaly and Munro, 1996]) and thus may represent a general feature of terminal differentiation. Given the substantial increase of MeCP2 expression accompanying this heterochromatic reorganization during myogenic differentiation and considering its preferential enrichment at pericentric heterochromatin (Fig. 1), we asked whether this increased concentration of MeCP2 could account for the observed changes in heterochromatin clustering.

## Ectopic expression of MeCP2-YFP induces clustering of pericentric heterochromatin independent of the histone H3K9 methylation pathway

To test whether MeCP2 plays a role in the aggregation of chromocenters, we transfected mouse myoblasts with a MeCP2-YFP fusion construct (Fig. 3, A and B) and performed a correlation analysis comparing expression levels of MeCP2-YFP with the number of chromocenters. 86 nuclei were first imaged for MeCP2-YFP fluorescence by confocal microscopy, followed by post-fixation and 3D-FISH with a major satellite-specific probe to visualize chromocenters. The correlation analysis revealed a significant ($P < 0.01$) negative correlation resulting in a coefficient of $-0.52$ (Fig. 3 D). Fig. 3 C shows two nuclei, one with low levels of MeCP2-YFP having many chromocenters (top), whereas the other (bottom), with high amounts of the fusion protein, shows only a few clusters. In addition to this reduction, also the variability in the number of chromocenters decreased with increasing MeCP2-YFP expression, similar to the results in differentiating myoblasts (Fig. 2). Control transfections using only YFP showed no effect on the clustering of chromocenters (see Fig. 6 B). Furthermore, expression of high levels of MeCP2 fused to other tags (GFP or DsRed variants) showed likewise clustering of chromocenters (see Fig. 6 A). To investigate whether other proteins with a similar nuclear localization as MeCP2 would be able to induce heterochromatin clustering, we transfected mouse myoblasts with constructs coding for fluorescently tagged versions of CENPB and HP1α. Although CENPB has been shown to localize at centromeric sites, in mouse chromosomes encompassing a region made up by the so-called minor satellite repeat (Amor et al., 2004), HP1α is mainly found in pericentric heterochromatin just as MeCP2, and represents one of the major constituents

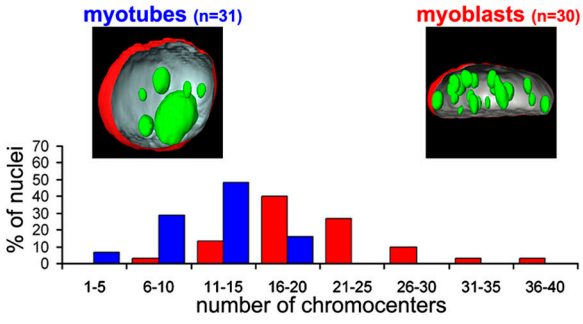


Figure 2. **Clustering of pericentric heterochromatin increases during myogenesis.** The histogram shows the number of chromocenters plotted versus the percentage of nuclei within populations of terminally differentiated myotubes (blue columns) and myoblasts (red columns). For each cell type, a 3D reconstruction of the TO-PRO3 nuclear counterstaining (red) and of pericentric heterochromatin labeled by a mouse major satellite-specific probe (green) is shown.

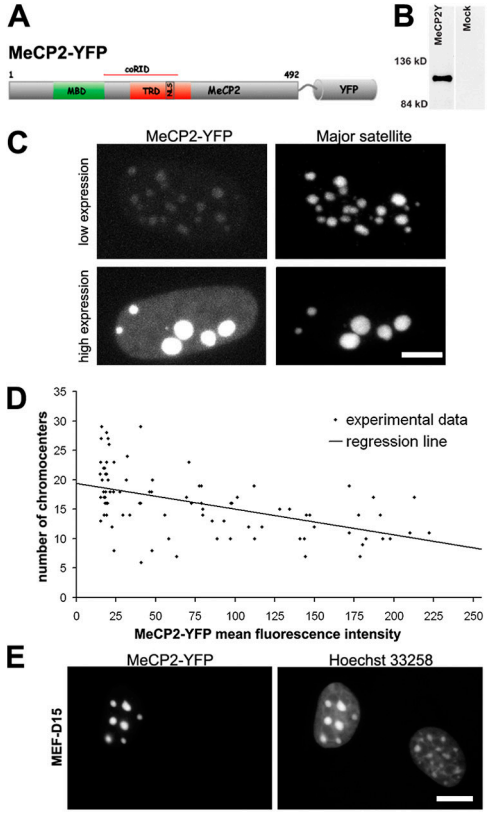


Figure 3. **MeCP2-YFP overexpression induces clustering of pericentric heterochromatin, which is independent of the histone H3 methylation pathway.** Pmi28 myoblasts growing on etched coverslips were transiently transfected with an MeCP2-YFP expression vector. Confocal image stacks of 86 nuclei with different expression levels were recorded using constant image acquisition parameters and their mean fluorescence intensity was calculated. After post-fixation and FISH using a major satellite-specific probe, pre-recorded nuclei were re-recorded to determine the number of chromocenters. (A) Rat MeCP2-YFP fusion protein and its functional domains (MBD, methyl CpG–binding domain; NLS, nuclear localization signal; TRD, transcriptional repression domain; coRID, corepressor interacting domain; numbers indicate amino acid positions). (B) Western blot with an anti-GFP antibody verifying expression of the fusion protein in transfected cells. (C) Images represent maximum intensity projections from confocal stacks of Pmi28 myoblasts expressing different levels of MeCP2-YFP. Bar, 5 μm. (D) The graph illustrates the results of the correlation analysis. The linear equation for the regression line was calculated as $y = -0.04 \times 19.41$. Panels in E show MEF-D15 suv39h1/2 double-null mouse fibroblasts transfected with MeCP2-YFP. Bar, 10 μm.

of constitutive heterochromatin (for review see Singh and Georgatos, 2003; Maison and Almouzni, 2004). In both cases we did not find an increased clustering of chromocenters in cells expressing high levels of the fusion proteins (see Fig. 6 B and Fig. S2, available at http://www.jcb.org/cgi/content/full/jcb.200502062/DC1). These results clearly argue against a general intrinsic clustering potential of centromeric or heterochromatin-associated proteins when expressed at high concentrations.

Next, we tested whether MeCP2-inducible clustering of chromocenters would depend on the specific constitutive heterochromatin modification of histone H3 (i.e., tri-methylation of lysine 9) and its binding protein HP1. For that purpose, we transfected mouse MEF-D15 fibroblasts (deficient for both histone H3 methyltransferases Suv39h1 and Suv39h2; Peters et al., 2001) with MeCP2-YFP. Both enzymes are responsible for trimethylation of histone H3 at lysine 9 at pericentric heterochromatin, which was shown to create a binding site for HP1 (Lachner et al., 2001). Transfected mutant cells exhibiting high levels of MeCP2-YFP showed an increased clustering of chromocenters despite lacking Suv39h1/2, histone H3K9 tri-methylation, and HP1 at pericentric sites (Fig. 3 E and Fig. S3, available at http://www.jcb.org/cgi/content/full/jcb.200502062/DC1), showing that the aggregation mechanism is independent from the HP1/H3K9 tri-methylation pathway.

Our experiments show that increased clustering of pericentric heterochromatin can be artificially induced by ectopic expression of MeCP2 in the absence of differentiation. These results indicate that the increased expression of endogenous MeCP2 during terminal differentiation (Fig. 1) is sufficient for inducing the observed aggregation of pericentric heterochromatin.

## Fusion of chromocenters occurs throughout interphase

Earlier reports have suggested a cell cycle–dependent redistribution of centromeric regions within the nucleus (Manuelidis, 1985; Vourc'h et al., 1993). We therefore investigated when during the cell cycle the fusion of chromocenters would take place. For that purpose, we doubly transfected C2C12 myoblasts with MeCP2-YFP and DsRed-Ligase I (Fig. 4 A) as a live-cell cell cycle progression marker (Easwaran et al., 2004, 2005). S-phase cells could be recognized simply by the subnuclear pattern of DsRed-Ligase I–labeled DNA replication foci (Cardoso et al., 1997; Leonhardt et al., 2000), whereas mitotic cells could be identified by chromosome condensation. G1 cells were identified by a previous mitosis or by a subsequent S-phase and G2 cells by a previous S-phase or a successive mitosis (Fig. 4 C). Of 14 nuclei analyzed, 9 showed fusions of chromocenters (example in Fig. 4 B and Video 1, available at http://www.jcb.org/cgi/content/full/jcb.200502062/DC1). A total of 30 fusions could be traced, with 15 occurring in G2, 10 in G1, and 5 in S-phase (Fig. 4 D).

Our results thus show that MeCP2-YFP–induced chromocenter clustering occurs through all interphase stages. The number of chromocenters in daughter nuclei was similar to that in the respective mother nuclei or higher, ruling out extensive fusions by defective chromosome segregation during mitosis.

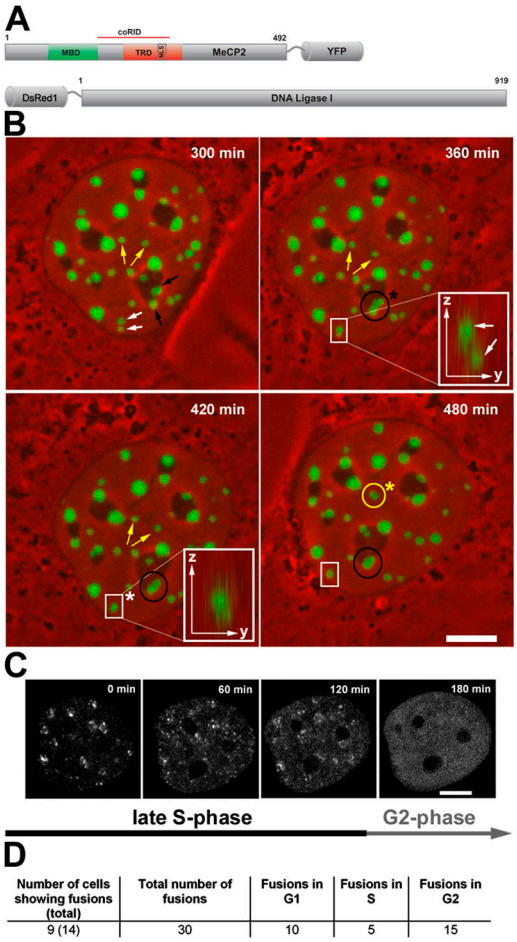


| Number of cells showing fusions (total) | Total number of fusions | Fusions in G1 | Fusions in S | Fusions in G2 |
|---|---|---|---|---|
| 9 (14) | 30 | 10 | 5 | 15 |

Figure 4. **Fusion of chromocenters occurs throughout interphase.** C2C12 myoblasts were double transfected with MeCP2-YFP and DsRed-Ligase I to track cell cycle progression. Schematic diagrams of the fusion proteins are depicted in A. (B) Maximum intensity projections generated from confocal image stacks of four time points of an MeCP2-YFP–transfected myoblast are shown (full time-lapse in Video 1, available at http://www.jcb.org/cgi/content/full/jcb.200502062/DC1). MeCP2-YFP is shown in green, phase-contrast images are in red. (C) As apparent from the DsRed-Ligase I replication pattern, this cell was in late S-phase and moved into G2 after 3 h. In B, the last 180 min from the time series are shown. Three fusion events are highlighted in different colors (yellow, white, and black). The time points where the actual fusions take place are marked by an asterisk and were analyzed in all three dimensions. Most observed fusions included very close chromocenters, but as in the case highlighted in yellow it could also affect chromocenters located >2 μm apart. Bar (B and C), 5 μm. The table in D summarizes the analysis from 14 time series. In 9 of these cells chromocenter fusions occurred.

Besides fusion events we also observed extensive splitting of heterochromatin clusters, occurring almost exclusively in G2 (Fig. S4 and Video 2, available at http://www.jcb.org/cgi/content/full/jcb.200502062/DC1). Hence, disruption of pericentric heterochromatin is likely to be an important prerequisite to perform mitosis properly.

## MeCP2-YFP–expressing cells exhibit enhanced chromocenter clustering during differentiation

Because MeCP2-YFP–transfected myoblasts were able to differentiate and many myotubes contained nuclei with high levels

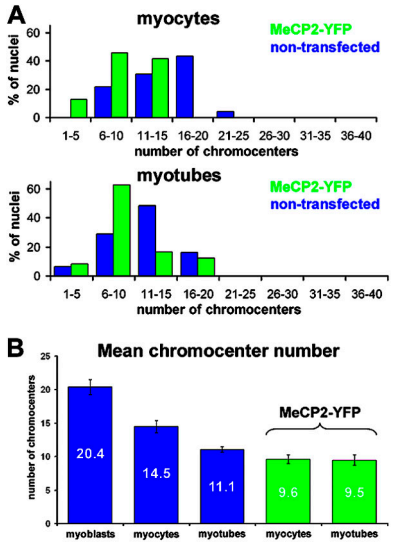


Figure 5. **Increased clustering during myogenic differentiation is enhanced by high MeCP2-YFP expression.** (A) The number of chromocenters in nontransfected Pmi28 myocytes and myotubes (blue columns) was compared with that in transfected Pmi28 myocytes and myotubes, which showed a substantial overexpression of MeCP2-YFP (green columns). In transfected cells, a clear shift toward a smaller number of clusters is evident. This effect is also visible if the mean number of chromocenters is compared (B). Myocytes, which represent an intermediate differentiation state between myoblasts and myotubes show also an intermediate number of chromocenters in nontransfected cells (blue). Error bars indicate SEM.

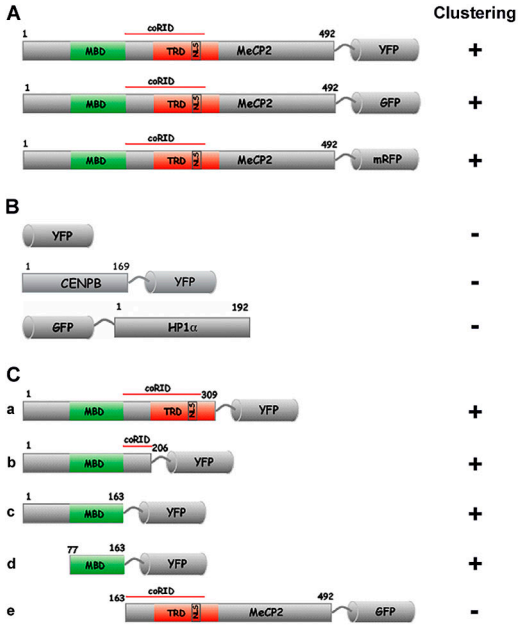


Figure 6. **The MBD is sufficient and necessary to induce clustering of pericentric heterochromatin I.** The sketch shows the structure of various fusion proteins that were expressed in mouse myoblasts in order to test for their clustering potential. + and − indicate whether or not an increased aggregation of pericentric heterochromatin could be observed in cells that showed high levels of the respective fusion protein. (A) Induced clustering by high MeCP2 expression could be observed irrespective of whether YFP, GFP, or the nonrelated DsRed derivative mRFP was used as a fluorescent tag. (B) Neither YFP alone nor the DNA-binding domain of the centromeric protein CENPB nor the pericentric heterochromatin protein HP1α appeared to induce clustering of pericentric regions (see also Fig. S2, available at http://www.jcb.org/cgi/content/full/jcb.200502062/DC1). (C) Truncated MeCP2 fusion proteins with increasing deletions of the COOH terminus (a–c) including the transcriptional repressor domain (TRD) and the corepressor interacting domain (coRID) were still able to induce chromocenter clustering. Clustering was even observed for a deletion mutant containing the MBD only (d). High level expression of an MeCP2 fusion protein lacking the $NH_2$ terminus including the MBD had no clustering effect (e), arguing that the MBD is necessary and sufficient for the induction of heterochromatin aggregation.

of the fusion protein, we conclude that overexpression of the protein in no way disturbs differentiation. When we compared the number of chromocenters in myotubes/myocytes showing a high MeCP2-YFP expression with that of nontransfected controls, we found significantly higher values in the control cells ($P < 0.01$ for myocytes and $P < 0.05$ for myotubes; Fig. 5 A). The mean number dropped from 14.5/11.1 in nontransfected myocytes/myotubes to 9.6/9.5 in transfected and highly expressing cells (Fig. 5 B). This means that high level of expression of MeCP2-YFP is not only compatible with the differentiation of transfected myoblasts, but it actually enhances pericentric heterochromatin clustering during terminal differentiation.

## The MBD of MeCP2 is sufficient and necessary to induce clustering of pericentric heterochromatin

At least three functional domains have been described for MeCP2; a methyl CpG–binding domain (MBD), a transcriptional repressor domain (TRD), and a corepressor interacting domain (coRID) (Fig. 3 and Fig. 6). The MBD comprises 85 amino acids, located at the $NH_2$-terminal end of the protein spanning amino acid positions 78–162 (Nan et al., 1993). This domain has been shown to be responsible for the interaction with methylated cytosines, and a single methylated CpG pair was shown to be sufficient for in vitro binding of the MBD (Lewis et al., 1992; Nan et al., 1993). The TRD extends from position 207 to 310 and was defined functionally by its ability to convey transcriptional repression upon transiently transfected reporter constructs (Nan et al., 1997). The NLS lies within the TRD at positions 255–271 (Nan et al., 1996). The coRID partially overlaps the TRD and extends $NH_2$ terminally until the MBD (aa 162). It was found to associate with the corepressor complex constituents mSin3A and the histone deacetylases HDAC1 and 2 (Nan et al., 1998), and consequently suggested to convey transcriptional silencing by recruiting chromatin-modifying complexes. Recently, a fourth domain at the COOH terminus has been described that apparently can interact with a domain found in splicing factors, though its function remains elusive (Buschdorf and Stratling, 2004).

To test whether a specific domain of the MeCP2 protein was responsible for the observed clustering of pericentric heterochromatin, we generated several truncated versions of MeCP2 tagged with a fluorescent protein and scored the clustering of chromocenters in cells expressing high concentrations of the mutated proteins (Fig. 6 C). In particular, we wanted to define whether the reported recruitment of histone deacetylase containing corepressor complexes by the coRID was needed for chromatin reorganization. All mutations having COOH-terminal deletions but retaining the MBD (Fig. 6

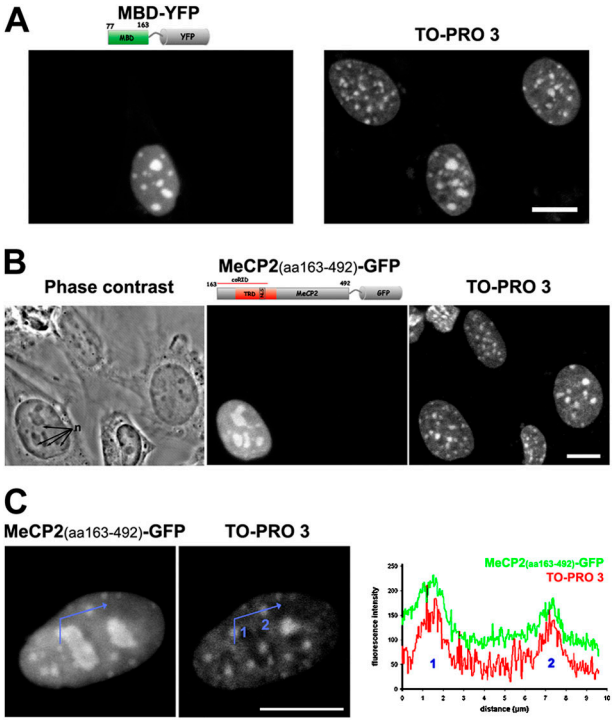


Figure 7. **The MBD is sufficient and necessary to induce clustering of pericentric heterochromatin II.** Pmi28 mouse myoblasts were transfected with several MeCP2 deletion mutants tagged with YFP or GFP. In the examples shown, cells were transfected with a vector containing only the MBD of MeCP2 fused to YFP (A), or with an MeCP2-GFP fusion lacking the first 162 amino acids including the MBD (B and C). A and B represent maximum intensity projections of confocal image stacks, except for the phase-contrast image, which is a mid-section. (C) Two mid-confocal sections. Bars, 10 μm. (A) Note that the cell expressing high levels of MBD-YFP exhibits a more pronounced clustering of chromocenters compared with nonexpressing cells, as revealed by TO-PRO 3 staining. (B) MeCP2-GFP lacking the $NH_2$ terminus (MeCP2(aa 163–492)-GFP) is highly concentrated in nucleoli (n) and did not induce chromocenter clustering. (C) Though lacking the MBD, the fusion protein still showed a preference for pericentric regions, although the contrast between nucleoplasmic and chromocenter staining is markedly reduced, compared with A. This preference for pericentric heterochromatin is also evident from the line scan plot. The blue line represents the track of the line scan; "1" and "2" mark chromocenter positions.

C, a–c) were able to induce clustering in mouse myoblasts, arguing against the necessity of the TRD, the coRID, and the most COOH-terminal portion of MeCP2 to induce aggregation of pericentric heterochromatin. In fact, a fusion construct consisting of the MBD alone was sufficient to cause chromocenter clustering in cells with high expression levels (Fig. 6 C, d; Fig. 7 A). In contrast, an $NH_2$-terminal deletion mutant lacking the MBD was not able to induce clustering, but instead showed a markedly increased staining of nonpericentric chromatin compared with the MBD-containing proteins, as well as an increased localization in nucleoli (Fig. 7 B). However, this fusion protein retained a clear preference to localize at pericentric sites (Fig. 7 C), arguing that the binding affinity of MeCP2 for major satellite regions is not exclusively dependent on the MBD.

Together, our deletion analysis clearly shows that the MBD is necessary and sufficient to induce clustering of chromocenters and is thus responsible for the observed clustering of pericentric regions in cells expressing high amounts of MeCP2.

## Clustering of pericentric heterochromatin occurs in muscle tissue of MeCP2-deficient mice

MeCP2 loss of function has been linked to the neurodevelopmental disorder Rett syndrome (Amir et al., 1999), in which maturation of neuronal cells seems to be impaired, possibly causing the severe neurological phenotype (for review see Kriaucionis and Bird, 2003). Concerning muscle development, Rett syndrome patients as well as MeCP2 knock-out mice (Guy et al., 2001; Shahbazian et al., 2002) show no severe defects (Jellinger, 2003).

To directly test whether MeCP2 is required for clustering of pericentric heterochromatin during mouse development, we compared chromatin topology in nuclei from muscle fibers of MeCP2 knock-out mice with that of control mice. Muscle fibers were stained with DAPI to highlight pericentric heterochromatin and to investigate chromocenter clustering (Fig. 8). Clustering of pericentric heterochromatin in skeletal muscle tissue of MeCP2-deficient mice was comparable to that in wild-type mice (Fig. 8) and in vitro differentiated myotubes (Fig. 2). These results clearly indicate that clusters of chromocenters can form in the absence of MeCP2, and we hypothesized that another member of the MBD protein family might be capable to reorganize chromocenters in a similar fashion as MeCP2.

## MBD2, but not MBD3, induces clustering of pericentric heterochromatin and, like MeCP2, its level increases during myogenic differentiation

MeCP2 belongs to a protein family that comprises at least five members, all of which share a functional MBD, besides MBD3, that is consequently incapable to specifically bind to methylated DNA (Hendrich and Bird, 1998). MBD2, like MeCP2, has been shown in transient transfection assays to localize preferentially at pericentric heterochromatin in a DNA methylation–dependent manner (Hendrich and Bird, 1998). Therefore, we tested if MBD2 could also induce chromocenter aggregation if expressed at high levels. Cells with high levels of an ectopically expressed GFP-MBD2 showed a significantly smaller number of chromocenters than nontransfected control cells (Fig. 9, A and B). Moreover, expression of endogenous MBD2 protein showed a stark increase during myogenic differentiation (Fig. 9 C), paralleling that of MeCP2 (Fig. 1 D). The observation that GFP-MBD2 can induce chromocenter clustering is in good agreement with the findings of our deletion analysis, showing that the MBD is sufficient to induce chromocenter clustering (Fig. 6 and Fig. 7). Indeed, we found also indications for an increased chromocenter clustering when we overexpressed GFP-tagged MBD1 and MBD4 (unpublished data), which also contain a functional MBD, and as assessed in transfection assays localize preferentially at pericentric sites (Hendrich and Bird, 1998). We also transfected mouse myoblasts with GFP-MBD3, which has been

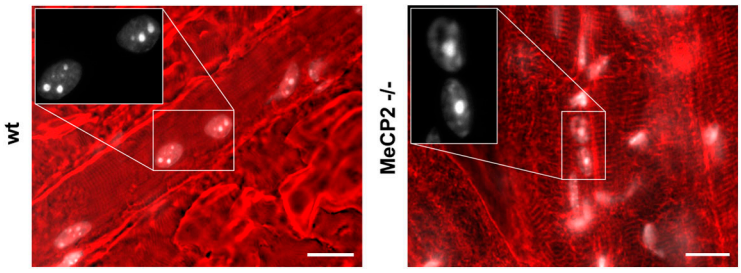


Figure 8. **Clustering of pericentric heterochromatin occurs in muscle tissue of wild-type mice as well as in MeCP2 knock-out mice.** Whole mouse myofibers from wild-type mice and MeCP2 null mice were fixed in formaldehyde and stained with DAPI to visualize myotube nuclei and chromocenters. Similar to in vitro–generated myotubes, a high fraction of nuclei showed an increased clustering of pericentric heterochromatin, i.e., chromocenters were large in size and few in number. In the widefield epifluorescent images shown, DAPI staining is in white and phase-contrast in red. Chromocenters are highlighted as intensely stained regions. Muscle fibers showed the characteristic striation by phase-contrast imaging, representing the sarcomeric organization. Bars, 20 μm.

shown to distribute diffusely in the nucleus with no preference for major satellite regions, if expressed at moderate levels (Hendrich and Bird, 1998). As expected, we found no indication for an increased chromocenter clustering in cells expressing high amounts of GFP-MBD3 (Fig. 9 D). Instead, we found an underrepresentation of GFP-MBD3 at pericentric sites (Fig. 9 E). A similar diffuse nucleoplasmic staining of MBD3 with a decreased concentration at major satellite regions was observed for the endogenous protein visualized by immunofluorescence in mouse myoblasts (unpublished data). Furthermore, MBD3 protein level did not show a significant increase during differentiation (Fig. 9 C).

Given the clustering potential of GFP-MBD2 and its increased expression level in differentiated myotubes, we conclude that MBD2 can substitute for MeCP2 in MeCP2 knock-out mice (Fig. 8), indicating a functional redundancy.

## Discussion

Our data provide evidence that aggregation of pericentric heterochromatin is a general feature of terminally differentiating myotubes, and that this major reorganization of nuclear topology can be induced by MeCP2 and MBD2. Furthermore, this rearrangement of heterochromatin is independent of the histone H3 trimethylation pathway and can occur throughout interphase.

A possible mechanism to explain how increasing levels of MeCP2 and MBD2 may contribute to aggregation of heterochromatin could involve oligomerization of these proteins bound to chromatin. These factors are not likely to be involved in movements of chromocenters or other chromatin regions, per se, but rather act as a sort of "glue" stabilizing random encounters of chromocenters within the nucleus. This is supported by a recent report (Georgel et al., 2003) showing that MeCP2 has the ability to interconnect nucleosomal arrays in vitro, creating oligomers consisting of several units. The authors have proposed DNA–MeCP2–MeCP2–DNA or DNA–MeCP2–DNA bridges to be responsible for the observed chromatin condensation activity. Such a mechanism could account for the clustering of pericentric heterochromatin during terminal differentiation simply by an increased interconnection due to elevated MeCP2 levels bound to methylated DNA. In this respect it should be noted that recombinant MeCP2 treated with the cross-linkers glutaraldehyde or EGS did not support a self-association of MeCP2 monomers (Klose and Bird, 2004).



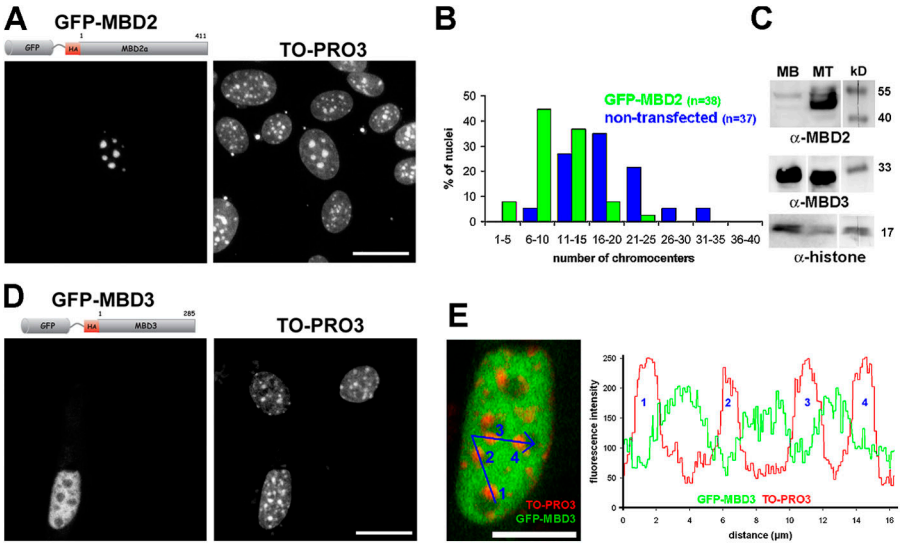


Figure 9. **MBD2 increases during myogenic differentiation and, in contrast to MBD3, binds to and induces clustering of pericentric heterochromatin in a dose-dependent manner.** Mouse myoblasts were transfected with GFP-MBD2 or GFP-MBD3 fusion constructs to test whether high expression levels of the fusion proteins would effect clustering of pericentric regions. In A and D, projection of confocal image stacks are shown. Bars, 20 μm. Note that the cell expressing high levels of GFP-MBD2 shows a remarkable increase in clustering of chromocenters as highlighted by TO-PRO counterstaining, whereas the nucleus with a high concentration of GFP-MBD3 shows an organization of pericentric heterochromatin, comparable to nonexpressing cells. Statistical analysis revealed that the number of chromocenters in cells expressing high levels of GFP-MBD2 is significantly reduced. The corresponding histogram in B illustrates the distinct distribution of chromocenter number of such cells (green) compared with nontransfected controls (blue). (C) Immunoblotting comparing endogenous levels of MBD2 and MBD3 in myoblasts versus myotubes. Histone concentrations were used as loading controls for nuclear proteins. (E) Mid-confocal section of the myoblast nucleus shown in D expressing high levels of GFP-MBD3. Bar, 10 μm. The blue line highlights the path of a line scan crossing four chromocenters (1–4, stained by TO-PRO3). The corresponding fluorescence intensity profile along the path shown in the plot demonstrates a decreased concentration of GFP-MBD3 in pericentric heterochromatin foci (fluorescent peaks at 1–4) and in the nucleolus.

However, it remains to be tested whether mouse MeCP2 is capable of forming multimers under other conditions, i.e., in a nuclear environment and bound to methylated satellite repeats.

Because MeCP2 and MBD2 are highly basic proteins (with pI ~10, similar to histones), they could act in a similar way as proposed for linker histones or inorganic bivalent cations (for review see Horn and Peterson, 2002) by neutralizing negative charges on the DNA, and thereby enabling or enhancing interactions between major satellite DNA located on separate chromocenters. Increased methylation of CpGs in pericentric regions (Fig. 1, C and E), creating a higher number of binding sites for MeCP2 and MBD2, would increase the probability of these proteins to bind, thereby augmenting their aggregation effect. However, the moderate degree of DNA methylation in the cell types analyzed suggests that extensive DNA methylation is not necessary for pericentric heterochromatin clustering. This is in agreement with a recent report showing that the compaction of oligonucleosomes by MeCP2 in vitro is not dependent on DNA methylation (Georgel et al., 2003).

Alternatively or in addition, a differentiation-dependent increase of MeCP2 could lead to a raise in the local concentration of histone deacetylases and/or of other chromatin-remodeling factors, which could bring about the observed aggregation effect. However, our results showing that the MBD domain alone, in the absence of the coRID, is sufficient for chromocenter reorganization (Fig. 6 and Fig. 7), argue against a role of the recruitment of deacetylase-containing complexes in the large-scale heterochromatin reorganization during differentiation. Also, the recently described recruitment of a histone H3K9 methylation activity by MeCP2 (Fuks et al., 2003) is unlikely to play a major role because mouse Suv39h double-null fibroblasts still showed increased clustering of pericentric heterochromatin upon MeCP2 overexpression, just as wild-type fibroblasts (unpublished data) or myoblasts did (Fig. 3 E). Altogether, our data favor a more direct and structural role of methyl CpG–binding proteins in chromatin reorganization rather than an indirect role through recruiting corepressor complexes.

Another aspect contributing to the clustering of pericentric heterochromatin in terminally differentiated, post-mitotic cells could be an intrinsic ability to aggregate during interphase, which in proliferating cells would be counteracted at each cell cycle by the dissociation of chromocenters as chromosomes condense and are separated during mitosis. With live-cell microscopy we could indeed follow such extensive dissociations of chromocenters in G2 nuclei before mitosis (Fig. S4 and Video 2). In post-mitotic, terminally differentiated cells, where chromosomes are no longer subjected to mitotic events, this "default" aggregation affinity would not be counteracted and might be further enhanced by MeCP2 and MBD2, finally leading to very large clusters.

A possible function of this nuclear reorganization of pericentric heterochromatin could be the establishment and/or stable maintenance of a specific transcriptional program in differentiated cells. The fact that heterochromatin, especially pericentric heterochromatin, conveys transcriptional silencing in many different settings, starting from position effect variegation (for review see Schotta et al., 2003) over transgene silencing (Francastel et al., 1999) to endogenous gene silencing (for review see Fisher and Merkenschlager, 2002), would support this hypothesis. It is conceivable that the silencing effects depend on a local threshold concentration of factors that are bound to or attracted by pericentric heterochromatin or some of its constituents. Forming bigger clusters would thus bring about an increase of such a critical concentration leading ultimately to the formation of effective silencing domains. Our results showing that MeCP2, which is known to act as a transcriptional repressor, plays an important role in inducing aggregation of heterochromatin clusters also favors this idea. Recently, it has been proposed that MeCP2 might be involved in the reduction of transcriptional noise (Hendrich and Tweedie, 2003). This function could be enhanced by a nuclear clustering that provides stringent control of leaky transcription via the creation of repressive subnuclear compartments. Moreover, our results showing that chromocenter clustering is maintained in MeCP2-deficient mice (Fig. 8) further strengthen the hypothesis that this large-scale topological chromatin reorganization might be of functional relevance, as it involves redundant pathways.

The finding that MeCP2 deficiency does not have a pronounced effect on gene expression pattern (Tudor et al., 2002) speaks in favor of MeCP2 being involved in stabilizing transcriptional silencing in terminally differentiated cells, rather than in regulating gene expression during differentiation. A recent report correlating the level of MeCP2 protein during central nervous system development in the mouse with the maturation of neurons further suggests that MeCP2 is involved in maintenance of the differentiated state, rather than in cell fate decisions (Kishi and Macklis, 2004). Alternatively, functional redundancy between MeCP2 and other methyl CpG–binding proteins such as MBD1 or MBD2, which have a similar pericentric distribution, could also explain the merely subtle changes in gene expression patterns observed in MeCP2-deficient mice (Tudor et al., 2002). Such a functional redundancy between MBD proteins is supported by our findings that MBD2 can likewise induce heterochromatin clustering and is expressed in a differentiation-dependent manner (Fig. 9). To which extent other MBDs can actually back up MeCP2 function has yet to be determined. Double or triple knockouts including MeCP2, MBD2, and MBD1 are required to further elucidate functional redundancies within the MBD protein family.

Both aspects of MeCP2 function (i.e., stabilization of transcriptional patterns and functional redundancy with other MBDs) would also explain why Rett syndrome patients as well as MeCP2 knock-out mice are viable and form differentiated tissues (for review see Kriaucionis and Bird, 2003), indicating that MeCP2 is not, per se, essential for cellular differentiation.

Our results clearly show that MeCP2 and MBD2 protein levels dramatically increase during differentiation and that either of them is sufficient to induce a large-scale chromatin reorganization during terminal differentiation, and thus represent a molecular link between nuclear genome topology and cellular differentiation.

## Materials and methods

### Plasmid constructs

The complete rat MeCP2 ORF as well as the DNA-binding domain of human CENPB (aa 1–169; Shelby et al., 1996) were fused in frame at the $NH_2$ terminus of the enhanced YFP (pEYFP-N1 vector; CLONTECH Laboratories, Inc.). The YFP-containing part from MeCP2-YFP fusion was cut out and replaced by either enhanced GFP (isolated from pEGFP-N1 vector; CLONTECH Laboratories, Inc.) or mRFP1 (Campbell et al., 2002) to construct MeCP2-GFP and MeCP2-mRFP1, respectively. MeCP2 deletion mutants were generated from the above plasmids using conveniently located restriction enzyme sites or by PCR amplification using primers including compatible restriction sites (primer sequences are available upon request). The complete human DNA ligase I ORF was fused in frame at the COOH terminus of the DsRed1 gene (pDsRed1-C1; CLONTECH Laboratories, Inc.) (Easwaran et al., 2004, 2005). The GFP-HP1α (human HP1α; Cheutin et al., 2003); GFP-MBD2 (human MBD2a; Tatematsu et al., 2000); MBD1-GFP, MBD4-GFP, and GFP-MBD3 (mouse cDNAs for MBD1, MBD4, and MBD3; Hendrich and Bird, 1998); and FLAG-HP1β (FLAG epitope–tagged mouse HP1β; Nielsen et al., 2001) were as described. Correct expression of all fusions in mammalian cells was checked by Western blot analysis as described before (Cardoso et al., 1997; Easwaran et al., 2005).

### Mouse tissue, cell culture, and transfection

Mouse muscle fibers from 50-d-old male MeCP2−/y (Guy et al., 2001) and from 12-wk-old male C57BL/6J used as controls were dissected from the hind limb and immediately frozen.

C2C12 mouse myoblasts and Pmi28 primary mouse myoblasts were cultured and differentiated as described previously (Cardoso et al., 1997; Kaufmann et al., 1999). The suv39h1/2 double-null and wild-type mouse fibroblasts (MEF-D15 and MEF-W9, respectively) were cultured as described before (Peters et al., 2001).

Pmi28 cells were transfected with PolyFect reagent (QIAGEN). For in vivo analysis, cells were transfected by the $Ca_3(PO_4)_2$ coprecipitation method as described previously (Cardoso et al., 1997).

To relocate MeCP2-YFP–expressing cells after post-fixation and FISH procedures, cells were cultivated on coverslips that featured 500 photoetched alphanumerical squares (Bellco). Myocytes were identified as postmitotic single nucleated cells in differentiated myotube cultures. To exclude cell cycle–dependent influences we included only S-phase cells for the evaluation of cycling myoblasts identified by pulse-labeling with BrdU (10 μM) 30 min before fixation. To determine post-mitotic cells, i.e., G0 cells, fixation was preceded by a 24-h BrdU (10 μM) incubation period. Details on BrdU detection can be found in Solovei et al. (2001).

### Western blotting

To compare the level of endogenous MeCP2, MBD2, and MBD3 protein in myoblasts versus myotubes, it was important to normalize for equivalent number of nuclei because myoblasts and myotubes have a very different cytoplasm/nucleus ratio and the methyl CpG–binding proteins are exclusively nuclear. For that purpose, DNA amounts from the different samples were measured using the Hoechst 33258 dye on a fluorimeter, and the arbitrary Hoechst fluorescence units from different cell suspension volumes were then compared to calculate equal nuclei amounts of cell suspension. Equivalent DNA-containing cell suspension aliquots were directly boiled in Laemmli loading buffer so that also insoluble proteins were solubilized and loaded onto the SDS-PAGE gels. This step was also relevant because methyl CpG–binding proteins are mostly bound to chromatin containing methylated DNA and therefore not efficiently extracted from the cells. MeCP2 was detected with a rabbit pAb (Abcam); MBD2 and MBD3 with a goat pAb (Santa Cruz Biotechnology, Inc.). Antibody specificity was tested by probing extracts of cells overexpressing tagged versions of all other family members with each individual antibody. Nuclear protein amounts were controlled by probing with an anti-histone mouse mAb (Roche clone H11-4).

### FISH and immunofluorescence

FISH with a mouse major satellite-specific probe was performed as described in Weierich et al. (2003). In brief, cells were fixed with 4% PFA in 1× PBS for myoblasts and in 0.75× PBS for myotubes. Cells were permeabilized with 0.5% Triton X-100/1× PBS followed by incubation in 20% glycerol and a repeated freezing/thawing step in liquid nitrogen. Additional pretreatments included incubation in 0.1 N HCl and for myoblasts/myotubes a pepsinization step.

The probe was generated by PCR using 5′-GCGAGAAAACTGAAAATCAC-3′ and 5′-TCAAGTCGTCAAGTGGATG-3′ as primers and mouse genomic DNA as template and labeled by nick translation using TAMRA-dUTP.

For immunofluorescence, cells were fixed as described for FISH until the Triton X-100 step. Mouse muscle fibers were fixed and permeabilized as cultured cells, but incubating 15 min for fixation and 40 min for permeabilization.

Detection of methylated DNA was performed as described previously (Habib et al., 1999). The following primary antibodies were used: rabbit anti-MeCP2 (Upstate Biotechnology) 1:25; mouse anti-5mC (Eurogentec) 1:100; goat anti-MBD3 (Santa Cruz Biotechnology, Inc.) 1:25; and mouse anti-FLAG M2 (Kodak) 1:2,000. As secondary antibodies we used goat anti–rabbit IgG-FITC (Sigma-Aldrich), goat anti–mouse IgG-Alexa 488 (Molecular Probes, Inc.), and donkey anti–goat IgG-Cy3 (Rockland).

Nuclear counterstaining was done using DAPI, Hoechst 33258, or TO-PRO 3. Samples were mounted in Vectashield antifade (Vector Laboratories).

### Southern blot

Genomic DNA from undifferentiated Pmi28 myoblasts and from differentiated cultures (6 d after application of differentiation medium) was isolated by spooling according to Sambrook and Russel (2001). Equal amounts of genomic DNA (5 μg) were digested overnight with the methylation-sensitive restriction enzyme HpyCH4 IV (5′-ACGT-3′) (New England Biolabs, Inc.), analyzed by 1.2% agarose gel electrophoresis, and blotted onto Zeta-Probe membrane (Bio-Rad Laboratories). A major satellite-specific probe was generated by PCR as described for FISH, whereas a PCR fragment corresponding to a repeat monomer was used, which was extracted by gel elution and labeled radioactively by random priming method (Prime-It II; Stratagene). After overnight hybridization, the membrane was washed and exposed to a phosphor screen. Signals were detected on a phosphorimager.

### Microscopy

Epifluorescence microscopy was performed at RT using an Axiophot 2 with 63×/1.4 oil and 100×/1.3 oil lenses (Carl Zeiss MicroImaging, Inc.), equipped with a Coolview CCD camera system (Photo Science Ltd.). Images were acquired with Cytovision software (Applied Imaging). Confocal image stacks were collected with an LSM410 and LSM510 microscope (Carl Zeiss MicroImaging, Inc.), equipped with 63×/1.4 oil and 63×/1.4 oil Ph3 lenses, respectively, at ambient temperature. For living-cell microscopy we used an FCS2 heated live cell observation chamber (Bioptechs) in combination with the Zeiss LSM510 microscope. The chamber was kept at a constant temperature of 37°C. The lateral resolution was between 0.05 and 0.1 μm. The axial resolution was between 0.2 and 0.5 μm in fixed cells and 0.75 μm in living cells. The temporal resolution of time series was 1 h.

### Image analysis and evaluations

Endogenous MeCP2 levels and methylation of cytosines visualized by immunofluorescence were evaluated by wide-field epifluorescence microscopy. The fraction of cells showing pericentromeric staining was determined by visual inspection.

Chromocenters were counted from confocal stacks using Image Browser software (Carl Zeiss MicroImaging, Inc.) by scanning the xy plane plus additionally inspecting z planes to discriminate between signals on top of each other.

Quantification of MeCP2-YFP fluorescence for the correlation analysis was done by determining the intranuclear mean fluorescence intensity of YFP using Image J software. As a first step, a threshold-defined counterstain-derived binary stack was created that defined the nuclear volume. This was used to set the signal intensity of all extranuclear voxels within the MeCP2-YFP channel to zero. All the remaining voxels were defined as intranuclear and their mean voxel intensity calculated.

Correlation analysis was performed using SPSS 11.5 software assuming a linear correlation. Differences between chromocenter numbers in different cell types were tested for statistical significance by comparing cumulative frequencies within individual cell populations using a two-sample Kolmogorov-Smirnov test.

Line scan analysis was performed on confocal mid-section images using LSM 5 Image Examiner software (Carl Zeiss MicroImaging, Inc.).

### Online supplemental material

Video 1 and Video 2 show dynamic behavior of pericentric heterochromatin in C2C12 mouse myoblasts visualized in vivo. Fig. S1 depicts chromocenter number during myogenic differentiation. Fig. S2 shows that high level expression of GFP-HP1α does not induce clustering of pericentric heterochromatin. Fig. S3 shows that HP1-β does not localize at pericentric

heterochromatin in Suv39h double-null fibroblasts. Fig. S4 depicts splitting of chromocenters in a G2 cell. Online supplemental material available at http://www.jcb.org/cgi/content/full/jcb.200502062/DC1.

Pmi28 myoblasts were provided by A. Starzinski-Powitz (Johann Wolfgang Goethe-Universität, Frankfurt Am Main, Germany) and suv39h1/2 double-null mouse fibroblasts by T. Jenuwein (IMP, Vienna, Austira). We thank T. Misteli (National Cancer Institute, Bethesda, MD) for GFP-HP1α plasmid; F. Ishikawa (Tokyo Institute of Technology, Tokyo, Japan) for GFP-MBD2a plasmid; R. Tsien (University of California, San Diego, San Diego, CA) for mRFP1 cDNA; P. Chambon (CNRS/INSERM/ULP/College de France, Illkirch, France) for FLAG-HP1β plasmid; and K. Sullivan (The Scripps Research Institute, La Jolla, CA) for the CENPB DNA-binding domain. We are indebted to A. Bird (University of Edinburgh, Edinburgh, UK) for providing us with rat MeCP2 cDNA, mouse MBD1-4 GFP expression plasmids, and muscle tissue from MeCP2−/y mice. We are very grateful to P. Domaing and M. Fillies for excellent technical assistance.

This work was funded by grants from the Deutsche Forschungsgemeinschaft to T. Cremer, H. Leonhardt, and M.C. Cardoso.

Submitted: 10 February 2005
Accepted: 2 May 2005

## References

Amir, R.E., I.B. Van den Veyver, M. Wan, C.Q. Tran, U. Francke, and H.Y. Zoghbi. 1999. Rett syndrome is caused by mutations in X-linked MECP2, encoding methyl-CpG-binding protein 2. *Nat. Genet.* 23:185–188.

Amor, D.J., P. Kalitsis, H. Sumer, and K.H. Choo. 2004. Building the centromere: from foundation proteins to 3D organization. *Trends Cell Biol.* 14:359–368.

Beil, M., D. Durschmied, S. Paschke, B. Schreiner, U. Nolte, A. Bruel, and T. Irinopoulou. 2002. Spatial distribution patterns of interphase centromeres during retinoic acid-induced differentiation of promyelocytic leukemia cells. *Cytometry.* 47:217–225.

Bird, A.P., and A.P. Wolffe. 1999. Methylation-induced repression—belts, braces, and chromatin. *Cell.* 99:451–454.

Brown, K.E., S.S. Guest, S.T. Smale, K. Hahm, M. Merkenschlager, and A.G. Fisher. 1997. Association of transcriptionally silent genes with Ikaros complexes at centromeric heterochromatin. *Cell.* 91:845–854.

Buschdorf, J.P., and W.H. Stratling. 2004. A WW domain binding region in methyl-CpG-binding protein MeCP2: impact on Rett syndrome. *J. Mol. Med.* 82:135–143.

Campbell, R.E., O. Tour, A.E. Palmer, P.A. Steinbach, G.S. Baird, D.A. Zacharias, and R.Y. Tsien. 2002. A monomeric red fluorescent protein. *Proc. Natl. Acad. Sci. USA.* 99:7877–7882.

Cardoso, M.C., C. Joseph, H.P. Rahn, R. Reusch, B. Nadal-Ginard, and H. Leonhardt. 1997. Mapping and use of a sequence that targets DNA ligase I to sites of DNA replication in vivo. *J. Cell Biol.* 139:579–587.

Chaly, N., and S.B. Munro. 1996. Centromeres reposition to the nuclear periphery during L6E9 myogenesis in vitro. *Exp. Cell Res.* 223:274–278.

Cheutin, T., A.J. McNairn, T. Jenuwein, D.M. Gilbert, P.B. Singh, and T. Misteli. 2003. Maintenance of stable heterochromatin domains by dynamic HP1 binding. *Science.* 299:721–725.

Cohen, D.R., V. Matarazzo, A.M. Palmer, Y. Tu, O.H. Jeon, J. Pevsner, and G.V. Ronnett. 2003. Expression of MeCP2 in olfactory receptor neurons is developmentally regulated and occurs before synaptogenesis. *Mol. Cell. Neurosci.* 22:417–429.

Dernburg, A.F., K.W. Broman, J.C. Fung, W.F. Marshall, J. Philips, D.A. Agard, and J.W. Sedat. 1996. Perturbation of nuclear architecture by long-distance chromosome interactions. *Cell.* 85:745–759.

Easwaran, H.P., L. Schermelleh, H. Leonhardt, and M.C. Cardoso. 2004. Replication-independent chromatin loading of Dnmt1 during G2 and M phases. *EMBO Rep.* 5:1181–1186.

Easwaran, H.P., H. Leonhardt, and M.C. Cardoso. 2005. Cell cycle markers for live cell analyses. *Cell Cycle.* 4:453–455.

Fisher, A.G., and M. Merkenschlager. 2002. Gene silencing, cell fate and nuclear organisation. *Curr. Opin. Genet. Dev.* 12:193–197.

Francastel, C., M.C. Walters, M. Groudine, and D.I. Martin. 1999. A functional enhancer suppresses silencing of a transgene and prevents its localization close to centrometric heterochromatin. *Cell.* 99:259–269.

Fuks, F., P.J. Hurd, D. Wolf, X. Nan, A.P. Bird, and T. Kouzarides. 2003. The methyl-CpG-binding protein MeCP2 links DNA methylation to histone methylation. *J. Biol. Chem.* 278:4035–4040.

Furuta, K., E.K. Chan, K. Kiyosawa, G. Reimer, C. Luderschmidt, and E.M. Tan. 1997. Heterochromatin protein $HP1^{Hs\beta}$ (p25β) and its localization with centromeres in mitosis. *Chromosoma.* 106:11–19.

Georgel, P.T., R.A. Horowitz-Scherer, N. Adkins, C.L. Woodcock, P.A. Wade, and J.C. Hansen. 2003. Chromatin compaction by human MeCP2. Assembly of novel secondary chromatin structures in the absence of DNA methylation. *J. Biol. Chem.* 278:32181–32188.

Guy, J., B. Hendrich, M. Holmes, J.E. Martin, and A. Bird. 2001. A mouse Mecp2-null mutation causes neurological symptoms that mimic Rett syndrome. *Nat. Genet.* 27:322–326.

Habib, M., F. Fares, C.A. Bourgeois, C. Bella, J. Bernardino, F. Hernandez-Blazquez, A. de Capoa, and A. Niveleau. 1999. DNA global hypomethylation in EBV-transformed interphase nuclei. *Exp. Cell Res.* 249:46–53.

Hendrich, B., and A. Bird. 1998. Identification and characterization of a family of mammalian methyl-CpG binding proteins. *Mol. Cell. Biol.* 18:6538–6547.

Hendrich, B., and S. Tweedie. 2003. The methyl-CpG binding domain and the evolving role of DNA methylation in animals. *Trends Genet.* 19:269–277.

Horn, P.J., and C.L. Peterson. 2002. Molecular biology. Chromatin higher order folding—wrapping up transcription. *Science.* 297:1824–1827.

Hsu, T.C., J.E. Cooper, M.L. Mace, and B.R. Brinkley. 1971. Arrangement of centromeres in mouse cells. *Chromosoma.* 34:73–87.

Jellinger, K.A. 2003. Rett syndrome—an update. *J. Neural Transm.* 110:681–701.

Jung, B.P., D.G. Jugloff, G. Zhang, R. Logan, S. Brown, and J.H. Eubanks. 2003. The expression of methyl CpG binding factor MeCP2 correlates with cellular differentiation in the developing rat brain and in cultured cells. *J. Neurobiol.* 55:86–96.

Kaufmann, U., J. Kirsch, A. Irintchev, A. Wernig, and A. Starzinski-Powitz. 1999. The M-cadherin catenin complex interacts with microtubules in skeletal muscle cells: implications for the fusion of myoblasts. *J. Cell Sci.* 112:55–68.

Kishi, N., and J.D. Macklis. 2004. MECP2 is progressively expressed in post-migratory neurons and is involved in neuronal maturation rather than cell fate decisions. *Mol. Cell. Neurosci.* 27:306–321.

Klose, R.J., and A.P. Bird. 2004. MeCP2 behaves as an elongated monomer that does not stably associate with the Sin3a chromatin remodelling complex. *J. Biol. Chem.* 279:46490–46496.

Kosak, S.T., and M. Groudine. 2004. Form follows function: The genomic organization of cellular differentiation. *Genes Dev.* 18:1371–1384.

Kriaucionis, S., and A. Bird. 2003. DNA methylation and Rett syndrome. *Hum. Mol. Genet.* 12(Suppl. 2):R221–R227.

Lachner, M., D. O'Carroll, S. Rea, K. Mechtler, and T. Jenuwein. 2001. Methylation of histone H3 lysine 9 creates a binding site for HP1 proteins. *Nature.* 410:116–120.

LaSalle, J.M., J. Goldstine, D. Balmer, and C.M. Greco. 2001. Quantitative localization of heterogeneous methyl-CpG-binding protein 2 (MeCP2) expression phenotypes in normal and Rett syndrome brain by laser scanning cytometry. *Hum. Mol. Genet.* 10:1729–1740.

Leonhardt, H., and M.C. Cardoso. 2000. DNA methylation, nuclear structure, gene expression and cancer. *J. Cell. Biochem. Suppl.* 35:78–83.

Leonhardt, H., H.P. Rahn, P. Weinzierl, A. Sporbert, T. Cremer, D. Zink, and M.C. Cardoso. 2000. Dynamics of DNA replication factories in living cells. *J. Cell Biol.* 149:271–280.

Lewis, J.D., R.R. Meehan, W.J. Henzel, I. Maurer-Fogy, P. Jeppesen, F. Klein, and A. Bird. 1992. Purification, sequence, and cellular localization of a novel chromosomal protein that binds to methylated DNA. *Cell.* 69:905–914.

Maillet, L., C. Boscheron, M. Gotta, S. Marcand, E. Gilson, and S.M. Gasser. 1996. Evidence for silencing compartments within the yeast nucleus: a role for telomere proximity and Sir protein concentration in silencer-mediated repression. *Genes Dev.* 10:1796–1811.

Maison, C., and G. Almouzni. 2004. HP1 and the dynamics of heterochromatin maintenance. *Nat. Rev. Mol. Cell Biol.* 5:296–305.

Manuelidis, L. 1985. Indications of centromere movement during interphase and differentiation. *Ann. NY Acad. Sci.* 450:205–221.

Martou, G., and U. De Boni. 2000. Nuclear topology of murine, cerebellar Purkinje neurons: changes as a function of development. *Exp. Cell Res.* 256:131–139.

Mitchell, A.R. 1996. The mammalian centromere: its molecular architecture. *Mutat. Res.* 372:153–162.

Mullaney, B.C., M.V. Johnston, and M.E. Blue. 2004. Developmental expression of methyl-CpG binding protein 2 is dynamically regulated in the rodent brain. *Neuroscience.* 123:939–949.

Nan, X., R.R. Meehan, and A. Bird. 1993. Dissection of the methyl-CpG binding domain from the chromosomal protein MeCP2. *Nucleic Acids Res.* 21:4886–4892.

Nan, X., P. Tate, E. Li, and A. Bird. 1996. DNA methylation specifies chromosomal localization of MeCP2. *Mol. Cell. Biol.* 16:414–421.

Nan, X., F.J. Campoy, and A. Bird. 1997. MeCP2 is a transcriptional repressor with abundant binding sites in genomic chromatin. *Cell.* 88:471–481.

Nan, X., H.H. Ng, C.A. Johnson, C.D. Laherty, B.M. Turner, R.N. Eisenman, and A. Bird. 1998. Transcriptional repression by the methyl-CpG-binding protein MeCP2 involves a histone deacetylase complex. *Nature.* 393:386–389.

Nielsen, A.L., M. Oulad-Abdelghani, J.A. Ortiz, E. Remboutsika, P. Chambon, and R. Losson. 2001. Heterochromatin formation in mammalian cells: interaction between histones and HP1 proteins. *Mol. Cell.* 7:729–739.

Peters, A.H., D. O'Carroll, H. Scherthan, K. Mechtler, S. Sauer, C. Schofer, K. Weipoltshammer, M. Pagani, M. Lachner, A. Kohlmaier, et al. 2001. Loss of the Suv39h histone methyltransferases impairs mammalian heterochromatin and genome stability. *Cell.* 107:323–337.

Sambrook, J., and D.W. Russel. 2001. Molecular Cloning: A Laboratory Manual. Cold Spring Harbor Laboratory, Cold Spring Harbor, NY. 6.16–6.18.

Schotta, G., A. Ebert, R. Dorn, and G. Reuter. 2003. Position-effect variegation and the genetic dissection of chromatin regulation in *Drosophila*. *Semin. Cell Dev. Biol.* 14:67–75.

Shahbazian, M., J. Young, L. Yuva-Paylor, C. Spencer, B. Antalffy, J. Noebels, D. Armstrong, R. Paylor, and H. Zoghbi. 2002. Mice with truncated MeCP2 recapitulate many Rett syndrome features and display hyperacetylation of histone H3. *Neuron.* 35:243–254.

Shelby, R.D., K.M. Hahn, and K.F. Sullivan. 1996. Dynamic elastic behavior of α-satellite DNA domains visualized in situ in living human cells. *J. Cell Biol.* 135:545–557.

Singh, P.B., and S.D. Georgatos. 2003. HP1: facts, open questions, and speculation. *J. Struct. Biol.* 140:10–16.

Solovei, I., J. Walter, M. Cremer, F. Habermann, L. Schermelleh, and T. Cremer. 2001. FISH on three-dimensionally preserved nuclei. *In* FISH: A Practical Approach. J. Squire, B. Beatty, and S. Mai, editors. Oxford University Press, Oxford, UK. 119–157.

Solovei, I., N. Grandi, R. Knoth, B. Volk, and T. Cremer. 2004. Positional changes of pericentromeric heterochromatin and nucleoli in postmitotic Purkinje cells during murine cerebellum development. *Cytogenet. Genome Res.* 105:302–310.

Tatematsu, K.I., T. Yamazaki, and F. Ishikawa. 2000. MBD2-MBD3 complex binds to hemi-methylated DNA and forms a complex containing DNMT1 at the replication foci in late S phase. *Genes Cells.* 5:677–688.

Tudor, M., S. Akbarian, R.Z. Chen, and R. Jaenisch. 2002. Transcriptional profiling of a mouse model for Rett syndrome reveals subtle transcriptional changes in the brain. *Proc. Natl. Acad. Sci. USA.* 99:15536–15541.

Vourc'h, C., D. Taruscio, A.L. Boyle, and D.C. Ward. 1993. Cell cycle-dependent distribution of telomeres, centromeres, and chromosome-specific subsatellite domains in the interphase nucleus of mouse lymphocytes. *Exp. Cell Res.* 205:142–151.

Weierich, C., A. Brero, S. Stein, J. von Hase, C. Cremer, T. Cremer, and I. Solovei. 2003. Three-dimensional arrangements of centromeres and telomeres in nuclei of human and murine lymphocytes. *Chromosome Res.* 11:485–502.

Yaffe, D., and O. Saxel. 1977. Serial passaging and differentiation of myogenic cells isolated from dystrophic mouse muscle. *Nature.* 270:725–727.

**Index of Online Supplemental Material for**
**J. Cell Biol. 10.1083/jcb.200502062**
**Brero et al.**

• **Figure S1** Chromocenter number during myogenic differentiation.

• **Figure S2** High level expression of GFP-HP1α does not induce clustering of pericentric heterochromatin.

• **Figure S3** HP1-ß does not localize at pericentric heterochromatin in Suv39h double-null fibroblasts.

• **Figure S4** Splitting of chromocenters in a G2 cell.

• **Video 1** (1.1 MB) Dynamic behavior of pericentric heterochromatin in C2C12 mouse myoblasts visualized in vivo.

• **Video 2** (452 k) Dynamic behavior of pericentric heterochromatin in C2C12 mouse myoblasts visualized in vivo.

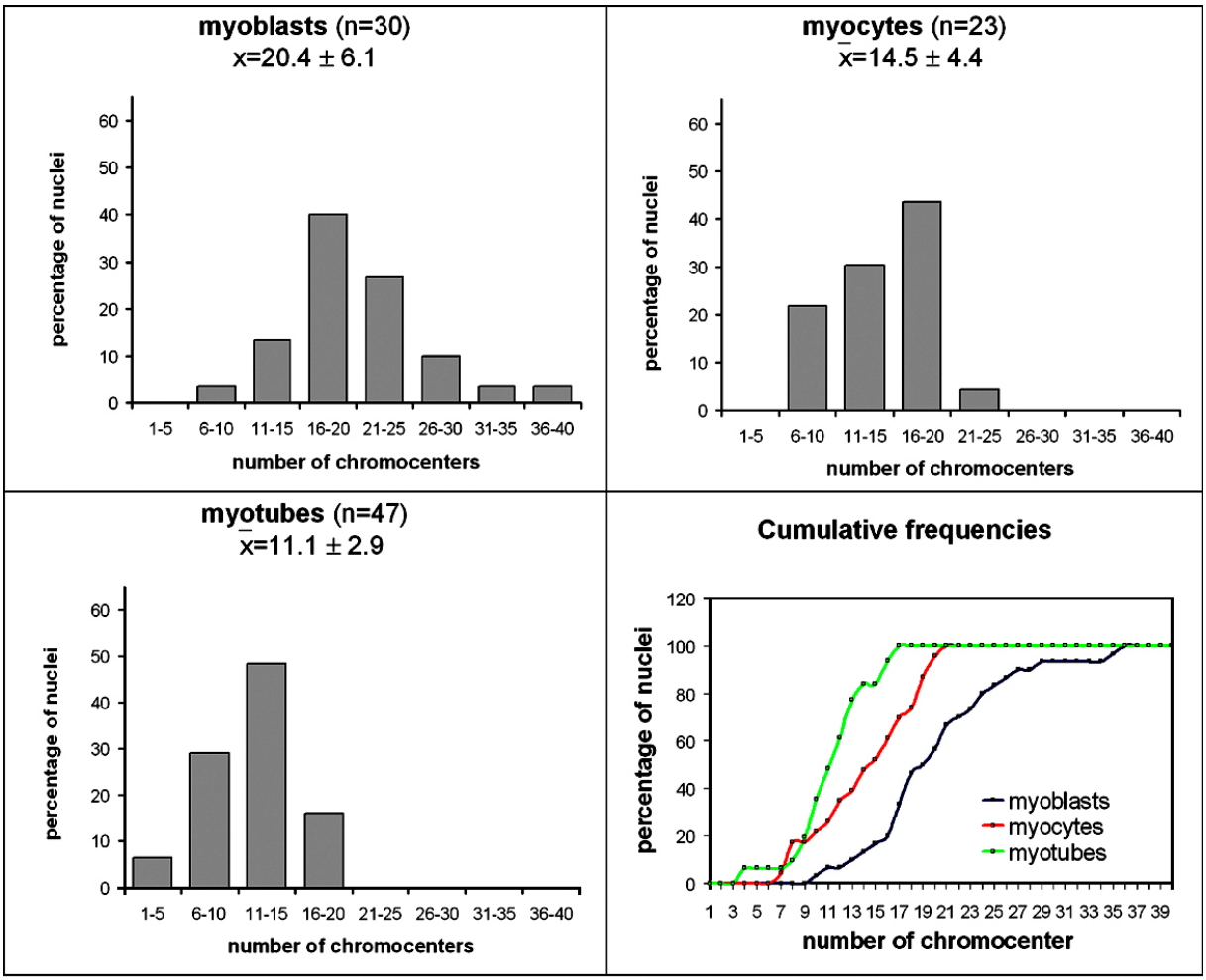


**Figure S1.** Chromocenter number during myogenic differentiation. Histograms illustrate the step-wise decrease in the chromocenter number from myoblasts over myocytes to finally myotubes. This gradual decline is mirrored by the average chromocenter number of the various cell types (x). Furthermore, the standard deviations also indicate a step-wise decrease in variability. The cumulative curves recapitulate this observation and illustrate comprehensively the results of the statistical analysis, which showed a significant decrease in the numbers of clusters from myoblasts to myocytes ($P < 0.05$) and to myotubes ($P < 0.001$), as well as from myocytes to myotubes ($P < 0.05$).

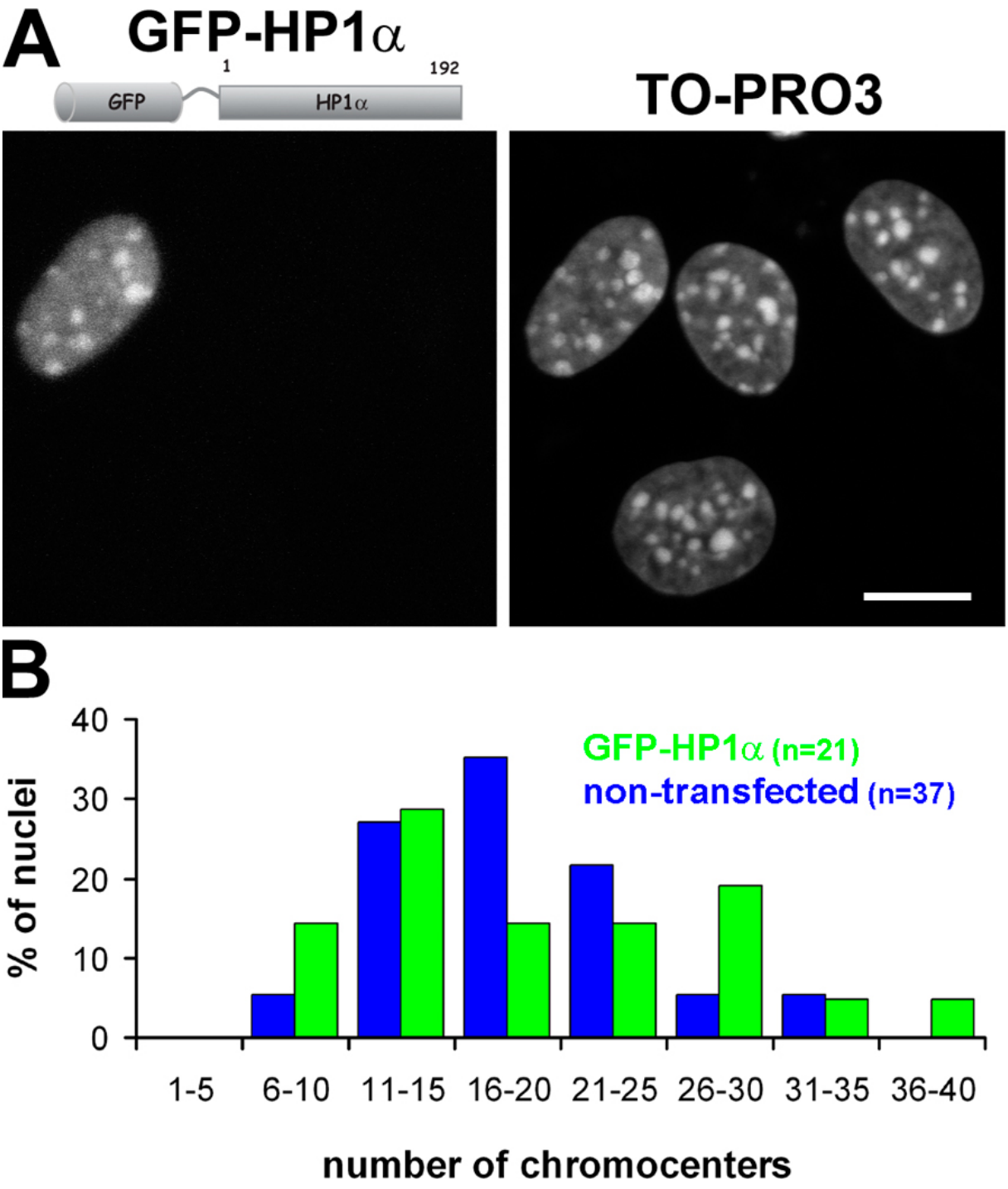


**Figure S2**. High level expression of GFP-HP1α does not induce clustering of pericentric heterochromatin. Pmi28 mouse myoblasts were transfected with GFP-HP1α, fixed, and stained with the DNA dye TO-PRO3, thereby highlighting pericentric heterochromatin. (A) Maximum intensity projections of confocal image stacks showing GFP-HP1α and TO-PRO3 fluorescence. Bar, 10 μm. Note that the nucleus showing a high expression of the HP1α fusion protein shows a similar number and size of chromocenters as nonexpressing cells. (B) Histogram illustrating the distribution of chromocenter number in cells with high GFP-HP1α concentrations versus nontransfected control cells. Statistical analysis revealed no significant differences between both cell populations ($P > 0.05$).

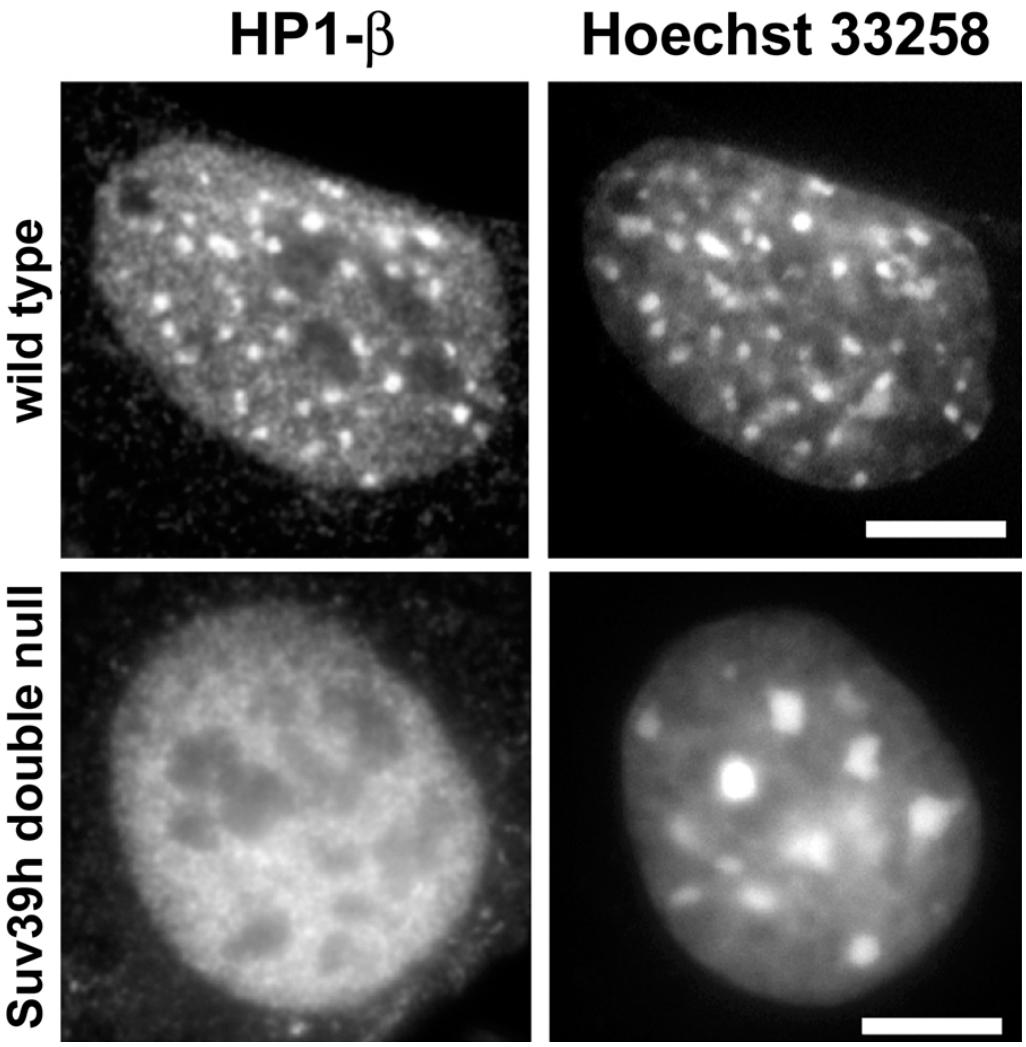


**Figure S3.** HP1-ß does not localize at pericentric heterochromatin in Suv39h double-null fibroblasts. Panels show epifluorescence images of wild-type MEF-W9 fibroblasts (top row) and of mutant MEF-D15 fibroblasts (bottom row) transfected with FLAG-tagged HP1ß expression plasmid (Nielsen, A.L., M. Oulad-Abdelghani, J.A. Ortiz, E. Remboutsika, P. Chambon, and R. Losson. 2001. Heterochromatin formation in mammalian cells: interaction between histones and HP1 proteins. Mol. Cell. 7:729-739.). HP1-ß was detected with anti-FLAG mouse antibody (left column) and DNA was counterstained with Hoechst 33258 (right column). MEF-D15 cells lack functional Suv39h1/h2 histone methyl transferases that are responsible for histone H3 lysine 9 tri-methylation (Peters, A.H., D. O'Carroll, H. Scherthan, K. Mechtler, S. Sauer, C. Schofer, K. Weipoltshammer, M. Pagani, M. Lachner, A. Kohlmaier, et al. 2001. Loss of the Suv39h histone methyltransferases impairs mammalian heterochromatin and genome stability. Cell. 107:323-337). The latter has been shown to be an HP1 binding site (Bannister, A.J., P. Zegerman, J.F. Partridge, E.A. Miska, J.O. Thomas, R.C. Allshire, and T. Kouzarides. 2001. Selective recognition of methylated lysine 9 on histone H3 by the HP1 chromo domain. Nature. 410:120-124; Lachner, M., D. O'Carroll, S. Rea, K. Mechtler, and T. Jenuwein. 2001. Methylation of histone H3 lysine 9 creates a binding site for HP1 proteins. Nature. 410:116-120). Consequently, Suv39h double-null fibroblasts lack H3K9 tri-methylation (not depicted), and do not show enrichment of HP1 at pericentric sites (bottom left), which are visualized as intensely stained regions by Hoechst 33258 (bottom right). In contrast, in wild-type cells all pericentric clusters show intense staining for HP1-ß.

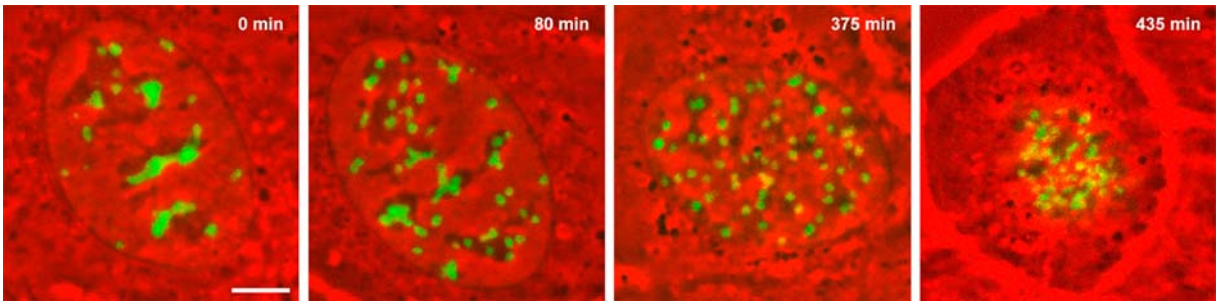


**Figure S4.** Splitting of chromocenters in a G2 cell. The images show a C2C12 mouse myoblast expressing MeCP2-YFP at selected time points of an in vivo time series. Maximum intensity projections of optical serial sections showing MeCP2-YFP (green) are combined with a mid-optical section (red) outlining the nuclear profile. Note that within 80 min many small chromocenters have already split from the larger "mother" clusters. By 60 min before mitosis almost all signals are small and similar sized, suggesting a separation of each chromosome's pericentric heterochromatin. Bar, 5 µm.

**Video 1**
Dynamic behavior of pericentric heterochromatin in C2C12 mouse myoblasts visualized in vivo. Cells were transiently transfected with MeCP2-YFP, highlighting pericentric heterochromatin clusters (green) and DsRed-Ligase for cell cycle stage determination (inset). Images were taken in 1-h intervals and are displayed at 0.5 frames/s. Fluorescent signals are shown as maximum intensity projections, while the nuclear outline (red) corresponds to a phase-contrast mid-confocal section. The time lapse captures the cell at the transition from late S-phase, with the big characteristic focal replication clusters revealed by DsRed-Ligase, to G2, where DNA Ligase I distributes homogenously in the nucleus. During a time course of 8 h, three chromocenter fusion events could be followed (color coded). Separate signals are highlighted by arrows (matched color); the fusion time points are marked by an asterisk. Note that single clusters labeled by two arrows represented two signals that were located above each other, so that in the projection view they appeared as one. Bar, 5 μm. The cell shown in the present movie corresponds to the cell shown in Fig. 4.

Video available at http://www.jcb.org/cgi/content/full/jcb.200502062/DC1/5

**Video 2**
Dynamic behavior of pericentric heterochromatin in C2C12 mouse myoblasts visualized in vivo. Cells were transiently transfected with MeCP2-YFP, highlighting pericentric heterochromatin clusters (green). Images were taken in 1-h intervals if not indicated otherwise (see insets of time points as h:min), and are displayed at 0.5 frames/s. MeCP2-YFP signals were 3D reconstructed from confocal optical serial sections using a surface rendering approach (Amira; TGS). The nucleus is outlined by a phase-contrast confocal mid-plane shown as transparent image (MeCP2-YFP signals beneath the phase-contrast section appear in a lighter green). During the first 2 h of observation several chromocenter fusions could be traced (color-coded arrowheads). In the 2 h preceding mitosis, signals increasingly changed their shape from ovoid/spherical to elongated irregular structures. Moreover, abundant chromocenter splitting could be observed, consequently leading to an increased chromocenter number. Confocal image stacks were aligned in the xy plane before reconstruction in order to correct for nuclear and cellular movements (therefore the phase-contrast images appear twisted).

Video available at http://www.jcb.org/cgi/content/full/jcb.200502062/DC1/6